

Two threefold interpenetrated two-dimensional frameworks based on a flexible imidazole-containing ligand and benzene-1,4-dicarboxylate

Ning-Ning Yuan, Qi-Kui Liu, Jian-Ping Ma, Ru-Qi Huang and Yu-Bin Dong*

College of Chemistry, Chemical Engineering and Materials Science, Key Laboratory of Molecular and Nano Probes, Engineering Research Center of Pesticide and Medicine Intermediate Clean Production, Ministry of Education, Shandong Provincial Key Laboratory of Clean Production of Fine Chemicals, Shandong Normal University, Jinan 250014, People's Republic of China

Correspondence e-mail: yubindong@sdu.edu.cn

Received 4 January 2011

Accepted 11 March 2011

Online 17 March 2011

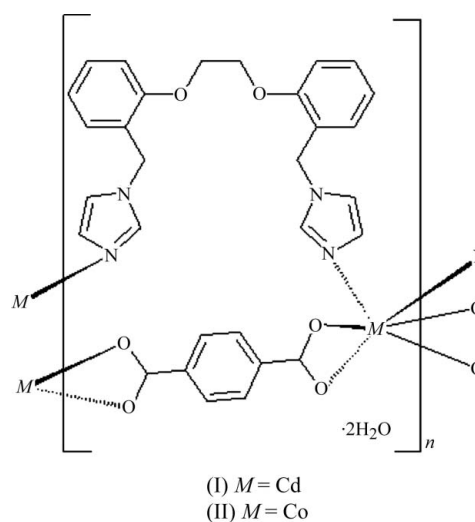
The open-chain polyether-bridged flexible ligand 1,2-bis[2-(1*H*-1,3-imidazol-1-ylmethyl)phenoxy]ethane (*L*) has been used to create two two-dimensional coordination polymers under hydrothermal reaction of *L* with Cd^{II} or Co^{II}, in the presence of benzene-1,4-dicarboxylic acid (H₂bdc). In poly[[$(\mu_2$ -benzene-1,4-dicarboxylato){ μ -1,2-bis[2-(1*H*-1,3-imidazol-1-ylmethyl)phenoxy]ethane}cadmium(II)] dihydrate], {[Cd(C₈H₄O₄)(C₂₂H₂₂N₄O₂)]·2H₂O}_{*n*}, (I), and the cobalt(II) analogue {[Co(C₈H₄O₄)(C₂₂H₂₂N₄O₂)]·2H₂O}_{*n*}, (II), the Cd^{II} and Co^{II} cations are six-coordinated by four carboxylate O atoms from two different bdc²⁻ dianions in a chelating mode and two N atoms from two distinct *L* ligands. The metal ions, bdc²⁻ dianions and *L* ligands each sit across crystallographic twofold axes. The bdc²⁻ coordination mode and the coordinating orientation of the *L* ligand play an important role in constructing the novel two-dimensional framework. Complexes (I) and (II) are threefold interpenetrated two-dimensional frameworks; their structures are almost isomorphous, while the bond lengths, angles and hydrogen bonds are different in (I) and (II).

Comment

The construction of coordination frameworks through crystal engineering has attracted considerable attention, not only because of their fascinating structure topologies (Abrahams *et al.*, 2004), but also due to their potential application as functional materials (Noveron *et al.*, 2002). In principle, some control over the type and topology of the polymer generated from the self-assembly of organic ligands and inorganic metal ions can be achieved by consideration of the functionality of the ligand (Munakata *et al.*, 1997). Flexible *N*-donor ligands

are good candidates for the assembly of versatile structures, owing to their diversity (Qi, Luo *et al.*, 2008). Such ligands incorporating imidazole are very useful organic building blocks for constructing metal–organic frameworks (MOFs), with many intriguing varieties of interpenetrating architectures and topologies (Cui *et al.*, 2005). Organic aromatic polycarboxylate ligands, especially benzene-1,4-dicarboxylic acid (H₂bdc), have been extensively applied in the construction of a rich variety of MOFs because of their diverse coordination modes and high structural stability (Lan *et al.*, 2009).

Recently, we reported several polymers generated from two novel flexible open-chain polyether-bridged organic ligands (Dong *et al.*, 2007; Jiang *et al.*, 2009). To research the coordination chemistry of the flexible open-chain polyether-bridged ligands with imidazole and a rigid aromatic polycarboxylate acid, we synthesized the novel ligand 1,2-bis[2-(1*H*-1,3-imidazol-1-ylmethyl)phenoxy]ethane (*L*) and investigated the self-assembly of *L* with Cd^{II} and Co^{II} under hydrothermal conditions in the presence of H₂bdc. Two MOFs with the same architectures and topologies were obtained, *viz.* {[Cd(bdc)(*L*)]·2H₂O}_{*n*}, (I), and {[Co(bdc)(*L*)]·2H₂O}_{*n*}, (II).



Complexes (I) (*M* = Cd) and (II) (*M* = Co) crystallize with one unique six-coordinated *M*^{II} centre. Each *M*^{II} cation sits on a twofold axis and has a distorted octahedral environment coordinated by four carboxylate O atoms [O2, O3, O2ⁱⁱⁱ and O3ⁱⁱⁱ; symmetry code: (iii) $-x + 1, y, -z + \frac{1}{2}$] from two bdc²⁻ dianions and two N atoms (N1 and N1ⁱⁱⁱ) from two *L* ligands. This coordination environment is similar to those observed in the structures of [Cd(oba)(1,4-bix)], (III), and [Co(bpea)(bbi)]·H₂O [oba is 4,4'-oxybis(benzoate), bpea is biphenylethene-4,4'-dicarboxylate, 1,4-bix is 1,4-bis(imidazol-1-ylmethyl)benzene and bbi is 1,1'-(1,4-butanediyl)bis(imidazole); Yang *et al.*, 2009]. The freedom of rotation around the central C–C single bond in *L* allows the ligand great conformational flexibility. In these structures, *L* adopts a twisted conformation (Figs. 1*a* and 1*b*). The O1–C11–C11ⁱ–O1ⁱ torsion angles [symmetry code: (i) $-x + 1, y, -z - \frac{1}{2}$] in *L* are -65.3 (6) and

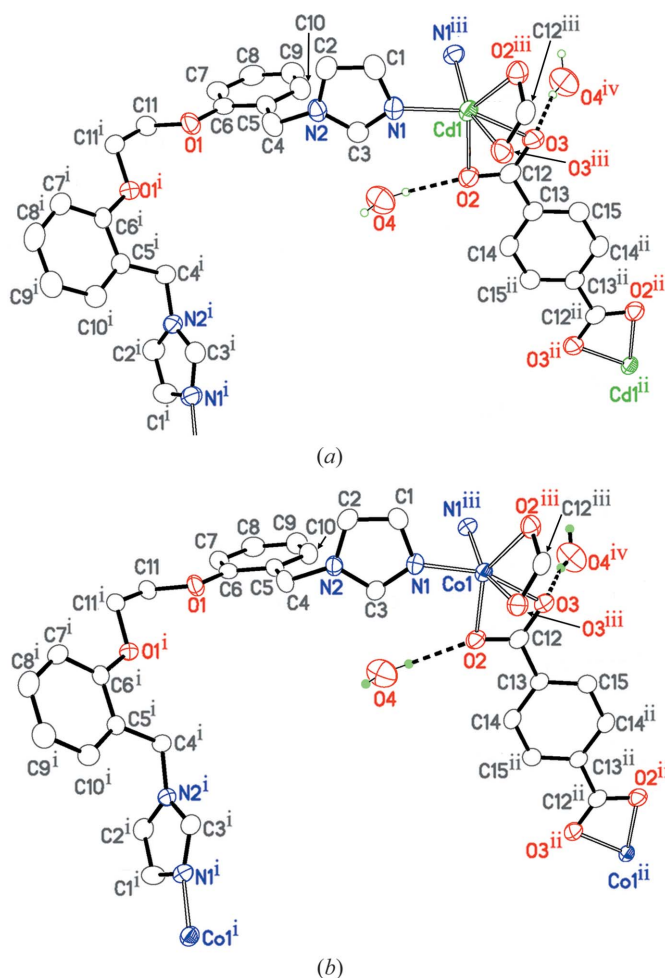


Figure 1
The molecular structures of (a) (I) and (b) (II), with displacement ellipsoids drawn at the 30% probability level. H atoms, except for those of the water molecule, have been omitted for clarity. [Symmetry codes: (i) $-x + 1, y, -z - \frac{1}{2}$; (ii) $-x + \frac{1}{2}, -y + \frac{3}{2}, -z$; (iii) $-x + 1, y, -z + \frac{1}{2}$; (iv) $x, -y + 2, z + \frac{3}{2}$.]

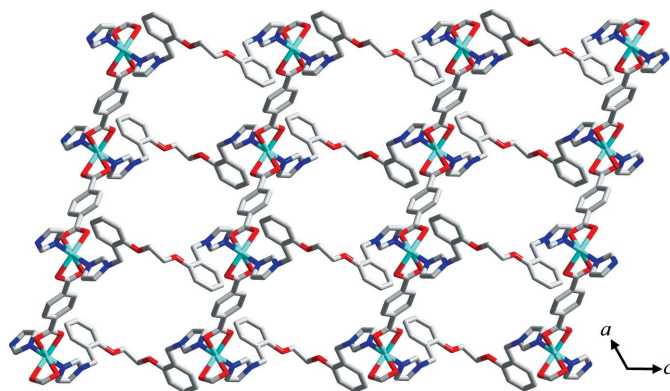


Figure 2
The two-dimensional wave-like sheet of (I).

$-69.4(5)^\circ$ in (I) and (II), respectively. The dihedral angles between the two terminal imidazole rings in *L* at the metal atom are $49.48(10)$ and $55.22(10)^\circ$, while the dihedral angles between the two benzene rings are $63.25(14)$ and $65.59(13)^\circ$

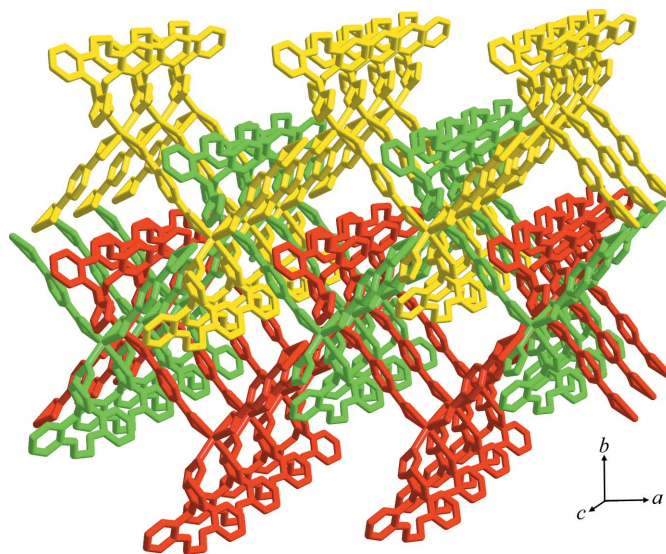


Figure 3
The two-dimensional parallel interpenetration of sheets in (I).

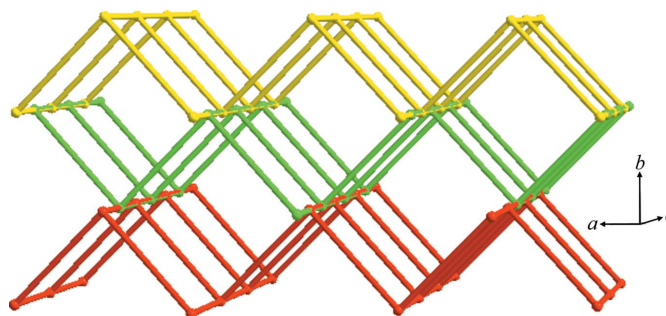


Figure 4
A schematic representation of the two-dimensional parallel interpenetration of sheets in (I).

in (I) and (II), respectively. All the *M*–O/N bond lengths are consistent with values reported for the *M*–carboxylate and *M*–imidazole complexes [Co(1,4-bdc)(*L*)] and [Cd₂(1,3-bdc)₂(*L*)₂] (Qi, Che *et al.*, 2008).

In the extended structures of (I) and (II), each *bdc*²⁻ dianion acts in a bis-bidentate chelating mode to bridge adjacent *M*^{II} cations to form zigzag one-dimensional chains. These chains are linked by *L* ligands into a two-dimensional wave-like sheet (Fig. 2) in the *ac* plane. Although a large four-membered ring formed by four Cd^{II} ions, two *L* ligands and two *bdc*²⁻ dianions exists in a single net, they are interpenetrated by other nets. These two-dimensional sheets are packed in the *ab* plane to form a threefold interpenetrated two-dimensional framework in a parallel fashion (Batten, 2001; Figs. 3 and 4). Each sheet is penetrated by two others (one above and one below) which have parallel but not coincident mean planes, leading to an overall three-dimensional entanglement architecture. The interpenetrated structure forms square channels when viewed down the *c* axis. Each square channel is formed by four *M*^{II} cations and four *bdc*²⁻ dianions and is filled by *L* ligands.

The water molecules are linked to the framework *via* O4—H4C···O3 and O4—H4D···O2($x, -y + 2, z - \frac{1}{2}$) hydrogen bonds. Although the two-dimensional framework topologies and the way they interpenetrate are similar to those in complex (III) (Yang *et al.*, 2009), there are some significant differences in their structures. In (III), there are interpenetrating channels and the nodes of adjacent sheets are parallel. For (I) and (II), however, there are square channels which are not interpenetrated, and the nodes of the adjacent sheets are in a line.

In summary, the most interesting feature in (I) and (II) is the presence of a threefold interpenetrated framework with square channels formed by *L* ligands and bdc²⁻ dianions. This behaviour may offer a route to new types of two-dimensional framework structures.

Experimental

For the preparation of ligand *L*, KOH (1.40 g, 25 mmol) was added, with stirring, to a solution of 1,2-bis(2-bromomethylphenoxy)ethane (2.00 g, 5 mmol) and imidazole (0.69 g, 10 mmol) in anhydrous tetrahydrofuran (50 ml) at ambient temperature. The mixture was stirred for 12 h at ambient temperature. After removal of the solvent under vacuum, the residue was purified on a silica-gel column using DCM–MeOH (20:1 *v/v*) as the eluent to afford *L* as a white crystalline solid (yield 1.07 g, 2.86 mmol, 57.6%). IR (KBr pellet, ν , cm^{-1}): 3094 (*m*), 2948 (*w*), 2884 (*w*), 1601 (*m*), 1589 (*m*), 1502 (*vs*), 1473 (*s*), 1453 (*s*), 1430 (*s*), 1388 (*w*), 1355 (*w*), 1339 (*w*), 1286 (*m*), 1247 (*vs*), 1223 (*s*), 1190 (*m*), 1156 (*w*), 1112 (*s*), 1087 (*s*), 1055 (*s*), 1039 (*m*), 908 (*w*), 840 (*w*), 814 (*s*), 774 (*s*), 751 (*vs*), 686 (*s*), 661 (*s*), 631 (*s*), 575 (*m*), 453 (*w*); ¹H NMR (300 MHz, CDCl₃, TMS): δ 7.50 (*s*, 2H, –C₃H₃N₂), 7.33 (*t*, 2H, –C₆H₄–), 7.07 (*d*, 2H, –C₆H₄–), 6.98 (*t*, 2H, –C₃H₃N₂), 6.97 (*t*, 2H, –C₆H₄–), 6.96 (*s*, 2H, –C₃H₃N₂), 6.90 (*s*, 2H, –C₆H₄–), 5.08 (*s*, 4H, –CH₂–), 4.30 (*s*, 4H, –CH₂–). Elemental analysis calculated for C₂₂H₂₂N₄O₂: C 70.59, H 5.88, N 14.97%; found: C 70.52, H 5.78, N 15.09%.

For the preparation of (I), *L* (3.74 mg, 0.01 mmol), Cd(NO₃)₂·4H₂O (3.08 mg, 0.01 mmol), H₂bdc (1.66 mg, 0.01 mmol) and water (2 ml) were sealed in a 5 ml glass tube. The mixture was heated at 453 K for 72 h under autogenous pressure. After the mixture had been allowed to cool to room temperature (over a period of 50 h), yellow bar-shaped crystals were isolated in 58.2% yield. IR (KBr pellet, ν , cm^{-1}): 3135 (*w*), 3120 (*w*), 2950 (*w*), 2930 (*w*), 2875 (*w*), 1625 (*m*), 1602 (*s*), 1544 (*vs*), 1495 (*s*), 1451 (*m*), 1438 (*m*), 1387 (*vs*), 1293 (*m*), 1252 (*s*), 1232 (*m*), 1175 (*w*), 1111 (*m*), 1086 (*s*), 1067 (*w*), 1052 (*w*), 1035 (*w*), 1013 (*w*), 942 (*m*), 886 (*w*), 840 (*s*), 750 (*vs*), 711 (*w*), 657 (*m*), 643 (*w*), 531 (*w*), 435 (*w*). Elemental analysis calculated for C₃₀H₃₀CdN₄O₈: C 52.45, H 4.40, N 8.16%; found: C 52.32, H 4.49, N 8.25%.

For the synthesis of (II), *L* (3.74 mg, 0.01 mmol), Co(NO₃)₂·6H₂O (3.37 mg, 0.01 mmol), H₂bdc (1.66 mg, 0.01 mmol) and water (2 ml) were sealed in a 5 ml glass tube. The mixture was heated at 423 K for 72 h under autogenous pressure. After the mixture had been allowed to cool to room temperature (over a period of 36 h), red crystals were isolated in 61.3% yield. IR (KBr pellet, ν , cm^{-1}): 3139 (*w*), 3124 (*w*), 2953 (*w*), 2931 (*w*), 2878 (*w*), 1627 (*m*), 1603 (*m*), 1546 (*vs*), 1495 (*s*), 1451 (*m*), 1438 (*m*), 1401 (*vs*), 1293 (*m*), 1252 (*s*), 1235 (*m*), 1179 (*w*), 1108 (*m*), 1088 (*m*), 1069 (*s*), 1053 (*w*), 1034 (*w*), 1013 (*w*), 946 (*m*), 886 (*w*), 837 (*m*), 750 (*vs*), 711 (*w*), 659 (*m*), 647 (*w*), 532 (*w*), 435 (*w*). Elemental analysis calculated for C₃₀H₃₀CoN₄O₈: C 56.88, H 4.77, N 8.84%; found: C 56.79, H 4.85, N 8.91%.

Table 1
Hydrogen-bond geometry (Å, °) for (I).

D—H···A	D—H	H···A	D···A	D—H···A
O4—H4D···O2	0.87	2.18	3.044 (4)	172
O4—H4C···O3 ^v	0.84	2.14	2.973 (4)	168

Symmetry code: (v) $x, -y + 2, z - \frac{1}{2}$.

Compound (I)

Crystal data

[Cd(C ₈ H ₄ O ₄)(C ₂₂ H ₂₂ N ₄ O ₂)]·2H ₂ O	$V = 2998 (3) \text{ \AA}^3$
$M_r = 686.98$	$Z = 4$
Monoclinic, $C2/c$	Mo $K\alpha$ radiation
$a = 17.450 (10) \text{ \AA}$	$\mu = 0.79 \text{ mm}^{-1}$
$b = 15.480 (8) \text{ \AA}$	$T = 298 \text{ K}$
$c = 12.636 (7) \text{ \AA}$	$0.26 \times 0.16 \times 0.09 \text{ mm}$
$\beta = 118.545 (7)^\circ$	

Data collection

Bruker SMART CCD area-detector diffractometer	8061 measured reflections
Absorption correction: multi-scan (SADABS; Bruker, 2003)	2944 independent reflections
$T_{\min} = 0.822, T_{\max} = 0.933$	2081 reflections with $I > 2\sigma(I)$
	$R_{\text{int}} = 0.034$

Refinement

$R[F^2 > 2\sigma(F^2)] = 0.040$	195 parameters
$wR(F^2) = 0.097$	H-atom parameters constrained
$S = 1.00$	$\Delta\rho_{\max} = 0.51 \text{ e \AA}^{-3}$
2944 reflections	$\Delta\rho_{\min} = -0.26 \text{ e \AA}^{-3}$

Compound (II)

Crystal data

[Co(C ₈ H ₄ O ₄)(C ₂₂ H ₂₂ N ₄ O ₂)]·2H ₂ O	$V = 2896.0 (10) \text{ \AA}^3$
$M_r = 633.51$	$Z = 4$
Monoclinic, $C2/c$	Mo $K\alpha$ radiation
$a = 17.612 (3) \text{ \AA}$	$\mu = 0.65 \text{ mm}^{-1}$
$b = 14.896 (3) \text{ \AA}$	$T = 298 \text{ K}$
$c = 12.711 (3) \text{ \AA}$	$0.26 \times 0.16 \times 0.09 \text{ mm}$
$\beta = 119.724 (3)^\circ$	

Data collection

Bruker SMART CCD area-detector diffractometer	7231 measured reflections
Absorption correction: multi-scan (SADABS; Bruker, 2003)	2547 independent reflections
$T_{\min} = 0.849, T_{\max} = 0.944$	1861 reflections with $I > 2\sigma(I)$
	$R_{\text{int}} = 0.049$

Refinement

$R[F^2 > 2\sigma(F^2)] = 0.052$	195 parameters
$wR(F^2) = 0.127$	H-atom parameters constrained
$S = 1.01$	$\Delta\rho_{\max} = 0.36 \text{ e \AA}^{-3}$
2547 reflections	$\Delta\rho_{\min} = -0.29 \text{ e \AA}^{-3}$

Table 2
Hydrogen-bond geometry (Å, °) for (II).

D—H···A	D—H	H···A	D···A	D—H···A
O4—H4D···O2	0.85	2.22	3.066 (4)	171
O4—H4C···O3 ^v	0.85	2.21	3.059 (4)	170

Symmetry code: (v) $x, -y + 2, z - \frac{1}{2}$.

H atoms attached to C atoms were placed in geometrically idealized positions and included as riding atoms, with C–H = 0.97 (CH₂) or 0.93 Å (CH) and $U_{\text{iso}}(\text{H}) = 1.2U_{\text{eq}}(\text{C})$. The water H atoms were located in a difference Fourier map, then their positions were constrained to ride on their parent atom with $U_{\text{iso}}(\text{H}) = 1.5U_{\text{eq}}(\text{O})$.

For both compounds, data collection: *SMART* (Bruker, 2003); cell refinement: *SMART*; data reduction: *SAINTE* (Bruker, 2003); program(s) used to solve structure: *SHELXS97* (Sheldrick, 2008); program(s) used to refine structure: *SHELXL97* (Sheldrick, 2008); molecular graphics: *SHELXTL* (Sheldrick, 2008); software used to prepare material for publication: *SHELXTL*.

This work was supported by the National Natural Science Foundation of China (grant Nos. 21072118 and 20871076) and Shandong Natural Science Foundation (grant No. JQ200803).

Supplementary data for this paper are available from the IUCr electronic archives (Reference: EM3039). Services for accessing these data are described at the back of the journal.

References

- Abrahams, B. F., Haywood, M. G., Hudson, T. A. & Robson, R. (2004). *Angew. Chem. Int. Ed.* **43**, 6157–6160.
- Batten, S. R. (2001). *CrystEngComm*, **3**, 67–72.
- Bruker (2003). *SADABS*, *SAINTE* and *SMART*. Bruker AXS Inc., Madison, Wisconsin, USA.
- Cui, G.-H., Li, J.-R., Tian, J.-L., Bu, X.-H. & Batten, S. R. (2005). *Cryst. Growth Des.* **5**, 1775–1780.
- Dong, Y.-B., Jiang, Y.-Y., Li, J., Ma, J.-P., Liu, F.-L., Tang, B., Huang, R.-Q. & Batten, S. R. (2007). *J. Am. Chem. Soc.* **129**, 4520–4521.
- Jiang, Y.-Y., Ren, S.-K., Ma, J.-P., Liu, Q.-K. & Dong, Y.-B. (2009). *Chem. Eur. J.* **15**, 10742–10746.
- Lan, Y.-Q., Li, S.-L., Fu, Y.-M., Du, D.-Y., Zang, H.-Y., Shao, K.-Z., Su, Z.-M. & Fu, Q. (2009). *Cryst. Growth Des.* **9**, 1353–1360.
- Munakata, M., Wu, L.-P., Kuroda-Sowa, T., Maekawa, M., Moriwaki, K. & Kitagawa, S. (1997). *Inorg. Chem.* **36**, 5416–5418.
- Noveron, J. C., Lah, M.-S., Del Sesto, R. E., Arif, A. M., Miller, J. S. & Stang, P. J. (2002). *J. Am. Chem. Soc.* **124**, 6613–6625.
- Qi, Y., Che, Y.-X., Luo, F., Batten, S. R., Liu, Y. & Zheng, J.-M. (2008). *Cryst. Growth Des.* **8**, 1654–1662.
- Qi, Y., Luo, F., Che, Y.-X. & Zheng, J.-M. (2008). *Cryst. Growth Des.* **8**, 606–611.
- Sheldrick, G. M. (2008). *Acta Cryst.* **A64**, 112–122.
- Yang, J., Ma, J.-F., Liu, Y.-Y. & Batten, S. R. (2009). *CrystEngComm*, **11**, 151–159.